Batteries & Supercaps

Research Article
doi.org/10.1002/batt.202400201

Chemistry Europe
European Chemical Societies Publishing

www.batteries-supercaps.org

State of Health Estimation of Lithium-ion Batteries Based on Machine Learning with Mechanical-Electrical Features

Lili Gong,[a] Zhiyuan Zhang,[a] Xueyan Li,[a] Kai Sun,[a] Haosong Yang,[a] Bin Li,[b] Hong Ye,[b] Xiaoyang Wang,[b] and Peng Tan*[a, c]

As one of the key parameters to characterize the life of lithium-ion batteries, the state of health (SOH) is of great importance in ensuring the reliability and safety of the battery system. Considering the complexity of practical application scenarios, a novel method based on mechanical-electrical feature extraction and machine learning is proposed to accurately estimate the SOH. A series of degradation experiments are designed to generate battery aging datasets, including the stress and voltage changes. Health features are directly extracted from the stress-voltage profile and the mechanical-electrical health feature factors are obtained through correlation analysis. The long short-term memory (LSTM) network is introduced to map the relationship between mechanical-electrical responses and the SOH, where the health feature factors are selected as input vectors. The effectiveness of the proposed method is demonstrated by battery datasets under different conditions, from which the estimated errors are less than 1.5%. This work demonstrates that the analysis and utilization of mechanical-electrical parameters can not only realize accurate SOH estimation, but also provide a broader field for battery energy management.

1. Introduction

The popularization of electric vehicles (EVs) is important to reduce carbon emissions, develop low-carbon economy, and promote energy transition. According to the International Energy Agency, EV sales in 2022 exceeded 10 million units.[1] Due to the advantages of high energy density and long cycle life, lithium-ion batteries have become the main energy storage devices for EVs. Hence, the monitoring and evaluation of lithium-ion battery status[2] are critical for early warning and avoiding safety accidents caused by battery degradation.[3] The state of health (SOH) is commonly defined by either capacity decay or increased internal resistance, which cannot be directly obtained by sensors. Therefore, it is urgent to establish high-precision, fast, and lossless SOH estimation methods.

A variety of SOH estimation methods have been developed from experiments, models, and data-driven analysis.[4–6] According to the definition of SOH, the experimental method requires strict test conditions and the test cycle is too long to be applied in online evaluation.[7] The model-based approach can characterize the internal electrochemical mechanism or the external electrical behavior of the battery with high accuracy. For example, a low-order electrochemical model with lithium-ion loss formation and crack propagation is developed for the use of online estimation techniques, which can predict capacity fade and voltage profile changes.[8] Nevertheless, the high computational complexity of the electrochemical model still limits its application in the battery management system (BMS). In contrast, the equivalent circuit model is simple to implement, requiring fewer parameters and less computational effort. Thus, most state estimation algorithms for EV applications are developed based on the equivalent circuit model. For example, Xiong et al. proposed a double-scale particle filtering method to estimate or predict the system state and parameters on two different time scales, where the akaike information criterion (AIC) is used to select a suitable battery model. Results showed that the proposed method was expected to be robust in practice and the application of AIC could achieve the balance of model prediction accuracy and complexity.[9] For a better understanding of battery aging mechanisms, a quick online estimation method with incremental capacity curves was presented,[10] which estimated the SOH by relating the location interval of two inflection points on differential voltage curves to battery capacity fade. Considering the advantages of signal analysis methods for extracting high-quality feature variables, an advanced filter algorithm is employed to obtain the smooth incremental capacity (IC) curves, then the dual Gaussian process regression (GPR) models are applied for the SOH estimation.[11] The effectiveness and robustness of the proposed model are demonstrated by four battery datasets with different health levels. For data-driven methods, the increasing dimension and size of input data may lead to information redundancy. Therefore, there are higher requirements for selecting data features and data training methods. Liu et al. proposed a multi-feature fusion model to estimate the SOH with support vector regression and long short-term memory network (LSTM).[12] In primary SVR models, the 5-fold cross-validation was adopted to deal with different feature parameters,

[a] L. Gong, Z. Zhang, X. Li, K. Sun, H. Yang, P. Tan
Department of Thermal Science and Energy Engineering, University of Science and Technology of China (USTC), Hefei 230026, Anhui, China
E-mail: pengtan@ustc.edu.cn

[b] B. Li, H. Ye, X. Wang
TacSense Technology Shenzhen Co., LTD, Shenzhen 518000, Guangdong, China

[c] P. Tan
State Key Laboratory of Fire Science, University of Science and Technology of China (USTC), Hefei 230026, Anhui, China
E-mail: pengtan@ustc.edu.cn

then the LSTM was used to fuse multiple primary SVR models to improve the performance of feature extraction. In contrast to previous feature extraction approaches, Goh et al. extracted health indicators with a U-chord curvature mode.[13] Three data-driven methods including GPR, LSTM, and back propagation neural network were used to ensure the estimation accuracy, reliability, and robustness. To solve the personalized battery usage preferences, Ma et al. developed a transfer learning framework for each end-user, where the cycling knowledge from cells with different usage protocols, charging-discharging configurations, and battery chemistries was employed.[14] Results showed that this approach obtained considerable generalizability in a variety of usage scenarios.

Although a lot of theoretical and experimental results have been achieved for the SOH estimation of lithium-ion batteries, numerous challenges still exist in applying these findings to real-world battery systems. At present, the BMS of EVs generally obtains battery status by monitoring the voltage, current, and temperature, and the corresponding estimation methods are also developed based on these three types of data. However, the mechanical stress that reflects the expansion characteristics of lithium-ion batteries is ignored regrettably. In reality, mechanical expansion significantly impacts battery performance,[15–17] which puts forward new requirements for battery management. As Li et al. summarized, the abundant electrochemical-mechanical coupled behaviors on the meso-scale or macroscale level are part of the reason for the failure to transfer the excellent performance of lithium-ion batteries at the laboratory/material scale to the industrial scale.[18]

Through a series of experiments, Cannarella et al. found that the capacity fade of constrained lithium-ion pouch cells under different pressure exhibits contrary cycle performance, and higher levels of mechanical stress would lead to higher rates of chemical degradation.[19] Furthermore, they conducted that the mechanical measurements during different cell operations presented a straightforward nature of the stress-SOH relationship, which provided a distinct advantage to the complicated models used for SOH estimation and battery management.[20] As the study of expansion behaviors at different scales, a phenomenological model was developed by Mohan et al. with an attempt to mimic the evolution of bulk force/stress and to quantify the contributions of intercalation and thermal expansion. Meanwhile, the feasibility based on the developed model for the state of charge (SOC) estimation was also highlighted.[21] Considering the good correspondence between the mechanical stress and the SOC, some attempts have been made in the SOC estimation.[22–24] Nevertheless, the application of stress measurements in the SOH estimation has not been well developed. Based on the incremental capacity analysis (ICA) method, Samad et al. used mechanical force instead of voltage to derive the IC curves.[25] They found that the noise of the force signal is much larger than the voltage signal and the proposed method could estimate the capacity fade of a battery at higher SOCs. In general, the standard capacity estimation method cannot identify each electrode's capacity and utilization window. Thus, a virtual model based on piecewise linear functions was introduced to identify the voltage and expansion parameters, which represented the electrode-specific SOH.[26] For future pack design, the mechanical behavior of high-capacity pouch cells was discussed, and then a model was proposed to estimate cell capacity fade under various compressive loads.[27] In terms of accuracy, Mohtat et al. explored the evolution of several features in the second differential of expansion that correlates to capacity loss and developed a capacity estimation method based on voltage and expansion.[28] Results show that the expansion measurement could enable fast and more robust capacity estimation during cycling testing in the lab. In terms of real conditions, Estevez et al. used mechanical stress measurement as a marker to assess the SOH.[29] Based on extensive experiments, they found that the cell pressure is linearly related to cell resistance and with a third-order polynomial to the SOH.

Although the relevance between mechanical stress and battery SOH has been well elucidated by the above works, the battery state estimation models and algorithms utilizing stress measurements are still in the early stage of development. To this end, this work fuses the mechanical and electrical signals for health feature extraction and introduces a machine-learning technique to estimate the SOH of pouch-type lithium-ion batteries. Based on sufficient aging tests, both stress and voltage changes are measured to analyze the degradation dynamics during the long-term cycle. The LSTM network is utilized for the SOH estimation, taking into account health feature factors such as stress and voltage characteristic parameters as input. With the aging datasets obtained from five batteries, the SOH estimation method is validated in different conditions. The contributions of this paper can be expressed as follows: 1) The mechanical stress is adopted to complement existing voltage-based estimation methods, which can uncover more sensitive information related to the SOH and provide a wider range of options for the estimation. 2) The proposed estimation method with an LSTM network can map battery mechanical-electrical signals directly to the SOH, avoiding complex modeling, parameter identification, and noise errors caused by data processing, which is suitable for actual EV applications. The paper is organized as follows: The methodology section details the experiment design, the health feature extraction, and the SOH estimation framework based on machine learning. The main outcomes of this research work are illustrated in the Results and Discussion section.

Methodology

Test Bench

Aging experimental datasets of five commercial lithium-ion pouch cells are used in this paper, and the details are listed in Table 1. The mechanical performance was tested on the tactile array system (Tacsense Technology, Shenzhen Co., LTD), and the parameters of the pressure sensor are shown in Table 2. The pressure acquisition system is equipped with a calibration function and can be drift-calibrated by an external device, ensuring the reliability of the stress data. The electrochemical performance was tested on a battery testing system (Neware, Shenzhen Co., LTD). All collected data were then transferred to a computer with MATLAB R2021a for post-analysis. The stress measurement is schemed in Figure 1.

Research Article
doi.org/10.1002/batt.202400201
Chemistry Europe
European Chemical Societies Publishing

Table 1. Information of the pouch-type lithium-ion battery.

Item	Parameter
Cathode	$LiNi_{0.88}Mn_{0.05}Co_{0.07}O_2$
Anode	SiO/C
Nominal capacity	14 Ah
Nominal voltage	3.55 V
Charge cut-off voltage	4.25 V
Discharge cut-off voltage Type	2.50 V
Size	150 mm×120 mm×5.2 mm
Specific energy	345 Wh kg^{-1}
Operating temperature	0~40 °C

Table 2. Information of the thin-film sensor.

Item	Parameter
Product model	SA6464–2525 A
Accuracy	>95 %
Thicknesses	<0.33 mm
Pressure range	4 MPa
Service life	>100,000 times
Repeatability	$<\pm5$ %
Nonlinearity	$<\pm3$ %
Operating temperature	−20 °C–85 °C

Aging Procedure

Before starting the cycling tests, the cells were discharged down to 2.5 V and held at rest for 0.5 h without any mechanical constraints to ensure electrochemical equilibrium. For cells 1 and 2, the aging cycling consists of a constant-current (CC), constant-voltage (CV) charging up to 4.25 V and cut-off at 0.05 C, followed by 0.5 h of relaxation, then a CC discharging until reaching 2.5 V for the full range conditions. For cell 3, an additional low current test (CC charging-discharging with a 0.05 C current) step was added after every 50 cycles. During all the tests, in addition to the traditional signals of voltage and current, the stress changes of the cell are also recorded. For cells 1 to 3, tests were done at room temperature. For cells 4 and 5, the test procedure was the same as cells 1 and 2 but conducted at a high temperature. The current adopted in this test was 1 C-rate.

Health Feature Extraction

Compared with the discharging process, the charging process contains stable and easily accessible information, which is convenient to carry out analysis. To avoid the impact on the model accuracy caused by the secondary processing of the data, the stress curves of the charging process were directly used for feature extraction. As the cycle proceeds, the characteristic parameters on the charging-discharging curve also keep changing. However, not all parameters have obvious and regular changes. Hence, it is necessary to select several parameters closely related to the battery performance degradation. The change in the voltage and stress curves during the charging-discharging process was depicted in Figure 2, and allow for the simplicity of the calculation process, this work chose five indicators as the health feature (HF) factors to estimate the battery SOH, namely:

1) HF1: Constant current charging time
2) HF2: Medium voltage
3) HF3: Maximum stress
4) HF4: Minimum stress
5) HF5: Maximum stress difference

Typically, the battery aging information can be reflected in the peak, average, slope, and area of the curve. Again, considering the applicability of the estimation method, the most easily accessible electrochemical characteristics (HF1, HF2) and mechanical characteristics (HF3, HF4, and HF5) were extracted here.

The Pearson correlation coefficient (ρ_{pe}) was employed to quantitatively evaluate the rationality of the selected health feature factors:[30]

$$\rho_{pe} = \frac{E(XS_{SOH}) - E(X)E(S_{SOH})}{\sqrt{E(X^2) - E^2(X)}\sqrt{E(S_{SOH}^2) - E^2(S_{SOH})}} \quad (1)$$

where X is the sequence of battery health feature factors, i.e., $X=$ [HF1, HF2, HF3, HF4, HF5] and $\rho_{pe} \in [-1, 1]$. The larger the absolute value of ρ_{pe}, the higher the degree of correlation.

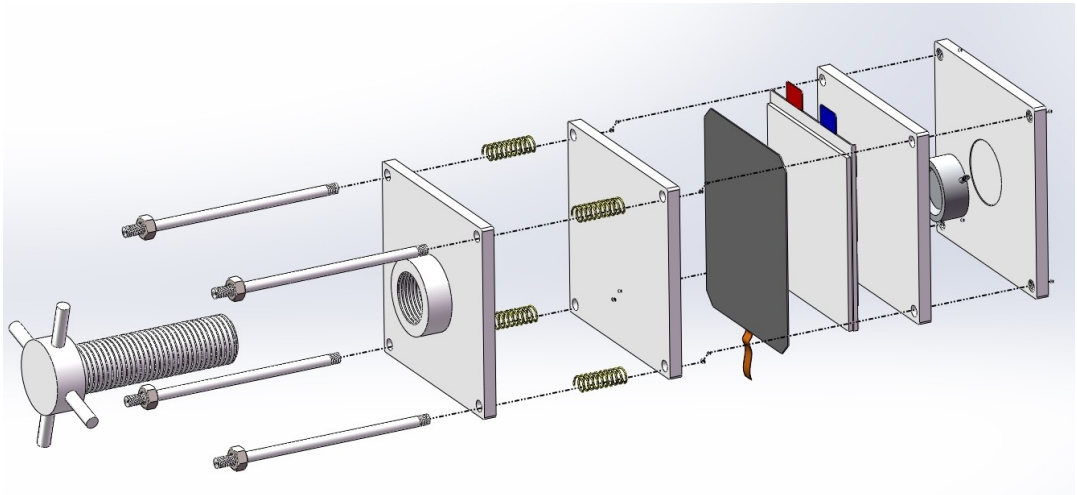

Figure 1. Scheme of the battery stress measurement system.

Research Article
doi.org/10.1002/batt.202400201
Chemistry Europe
European Chemical Societies Publishing

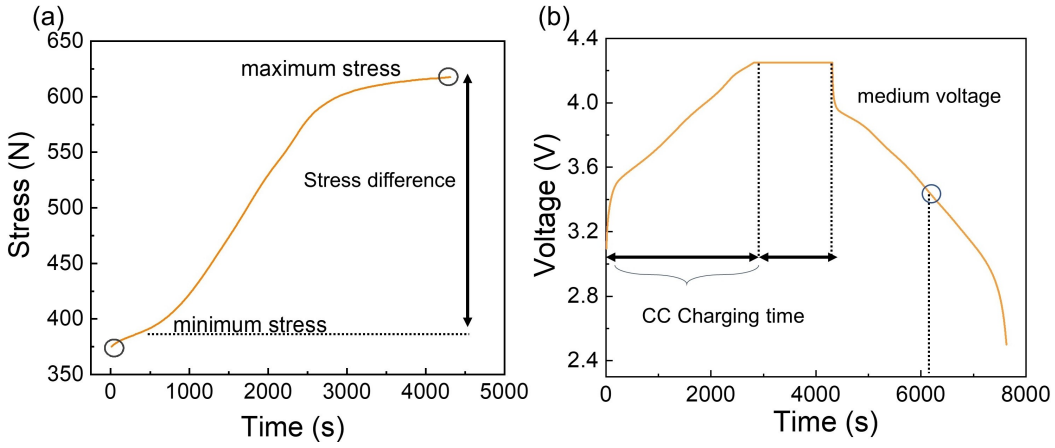

Figure 2. The change in the voltage and stress curves during the charging-discharging process. (a) Stress and (b) Voltage.

SOH Estimation Using LSTM

The SOH is defined as the ratio of the maximum available capacity to the nominal capacity using the following equation:

$$SOH = \frac{Q_c}{Q_n} \times 100\% \tag{2}$$

where Q_c is the maximum available capacity of the battery at the current cycle, Q_n is the nominal capacity of the battery.

The LSTM network is a type of recurrent neural network, which is particularly effective in processing and making predictions based on sequential data.[31] The key innovation of LSTM is the introduction of memory units, which allow the network to selectively store and access information over long periods. Each memory unit is made up of three main components: input gate, forget gate, and output gate. The information propagation of LSTM can be expressed as follows:[32]

$$\begin{cases} i_m = \sigma(W_i[h_{m-1}x_m] + b_i) \\ f_m = \sigma(W_f[h_{m-1}x_t] + b_f) \\ c_m = f_m c_{m-1} + i_t \tanh(W_c[h_{m-1}x_m] + b_c) \\ o_m = \sigma(W_o[h_{m-1}x_m] + b_o) \\ h_m = o_m \tanh(c_m) \end{cases} \tag{3}$$

where x_m is the LSTM unit, i_m, f_m, o_m, c_m, h_m represent the state of the input gate, forget gate, state unit, and LSTM result, respectively; $W = [W_i, W_f, W_c, W_o]$ and $b = [b_i, b_f, b_c, b_o]$ are the weight matrix and bias term, respectively; σ and tanh are the sigmoid activation function and double tangent activation function, respectively.

Given that the performance parameters of the battery during the aging test exhibit a clear long-time dependence, the LSTM network is introduced to estimate SOH. By capturing nonlinear relationships in battery data, a network with health feature factor as input and battery SOH as output is constructed. The flow chart of the proposed SOH estimation method for pouch lithium-ion batteries is shown in Figure 3, and the specific steps are summarized below:

1) Data collecting, obtain battery operating parameters during the aging process under preset operating conditions, including voltage, current, and stress.
2) Heath feature extraction, extract the relevant features according to the charging curves and analyze the correlation between feature factors and SOH.
3) Model training, divide the data into a training set and a test set, update the network using the training set.
4) SOH Estimation, three operation cases are performed using the test set.
5) Results Analysis, several error analysis methodologies are applied to assess the accuracy of the LSTM-based estimation method.

Data Processing

The data collected in Section 2.2 were used to clarify the necessity of mechanical stress for the SOH estimation, explore the feasibility of using stress characteristics for the SOH estimation, and verify the effectiveness of the proposed SOH estimation method. To ensure the comparability between evaluation indicators, the Min-Max normalization method was adopted to unify different types of data under one reference system. The *MAE*, *RMSE*, *MAPE*, and R^2 were all employed to evaluate the precision of SOH estimation and the degree of model fit, and their equations are expressed as follows:

$$MAE = \frac{1}{N}\sum_{n=1}^{N}\left|y_n - y_n\right| \tag{4}$$

$$MAPE = \frac{100\%}{N}\sum_{n=1}^{N}\left|\frac{y_n - y_i}{y_i}\right| \tag{5}$$

$$RMSE = \sqrt{\frac{1}{N}\sum_{n=1}^{N}\left(y_n - y_n\right)^2} \tag{6}$$

$$R^2 = 1 - \frac{\sum_{n=1}^{N}\left(y_n - y_n\right)^2}{\sum_{n=1}^{N}\left(y_- - y_n\right)^2} \tag{7}$$

Research Article
doi.org/10.1002/batt.202400201
Chemistry Europe
European Chemical Societies Publishing

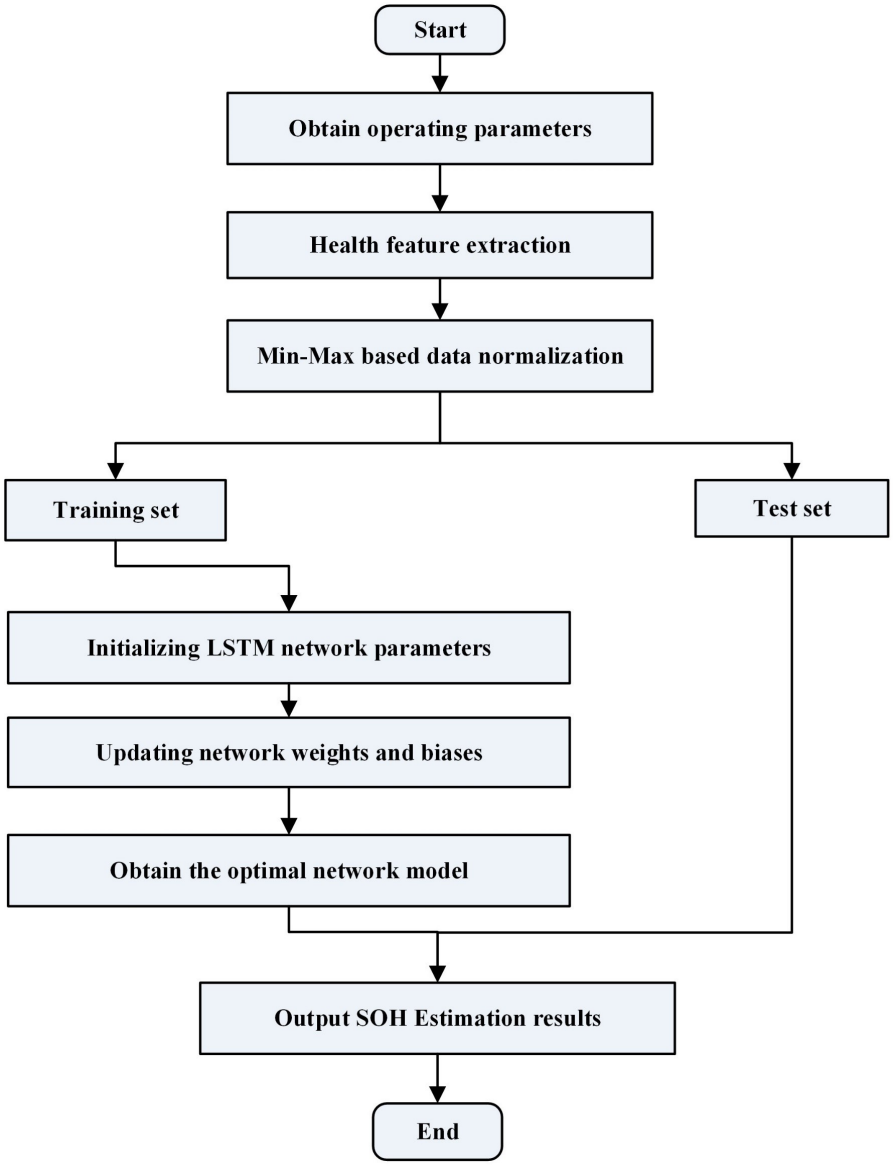

Figure 3. Flowchart of the SOH estimation method using LSTM.

where N is the total number of cycles in the test data set, y_n and $\hat{y}$ are the true and estimated values of the SOH; $\bar{y}$ is the average value of the true SOH; *MAE* is the evaluation of the average amplitude of model error, while *MAPE* uses percentages to measure the magnitude of deviations, which are easy to understand and interpret. *RMSE* is commonly used to measure the dispersion degree of model error. For *MAE*, *MAPE*, and *RMSE*, the smaller the index value is, the higher accuracy of the prediction model achieves. For *R2*, it should be a better model if the value is more than 0.8.

2. Results and Discussion

To analyze and validate the proposed SOH estimation method in this section, three operation cases were set as follows:

Case 1: The suggested method was validated using the datasets of cell 1.

Case 2: The suggested method was validated using the datasets of cell 2.

Case 3: Integrating the datasets of cell 1 and cell 2, then the suggested method was validated using the newly constructed dataset.

In the LSTM algorithm, the dataset is divided into the training set and the test set. The training set is used to train the model, continuously optimizing model parameters to improve its performance on the training data. Meanwhile, the test set is used to evaluate the final performance of the model, providing a true reflection of its generalization ability on new data. For cell 1, a total of 374 cycles were completed, while for cell 2, a total of 495 cycles were completed. To maintain consistency, the last 50 cycles are taken as the test set across all three cases in this article to validate the effectiveness of the proposed method. The neural layers of the LSTM neural network are set to 128, and the maximum number of iterations is 600. To

improve the convergence speed and accuracy of the LSTM network, the learning rate of linear decay is used in this paper. The initial learning rate is set as 0.005, and the learning rate drop factor is set as 0.1. After that, the durability and accuracy of the estimation method were discussed and an error analysis methodology was applied to evaluate the model performance.

2.1. Characteristic Curve Analysis

To highlight the importance of stress measurement in the SOH estimation, an assessment of the effect on battery capacity due to mechanical was provided. Meanwhile, a detailed analysis of mechanical-electrochemical characteristic curves was performed.

Figure 4(a) shows the capacity retention curves of the lithium-ion battery with and without preloading during cycles. It can be observed that the degradation trends are very different under two operating conditions, which indicates that the traditional SOH estimation results without considering the mechanical expansion characteristics are not consistent with practical applications. In view of the actual operating conditions of EVs, the stress variation shown in Figure 4(b) should also be considered in battery SOH estimation.

The voltage and stress variation at different number of cycles are shown in Figure 5. As the number of cycles increases, the overall stress grows larger, and the voltage curve is also shifting but not significantly.

Similar to the voltage variation, a differential analysis of the stress evolution was also carried out to further investigate the association between electrochemical and mechanical responses. Figure 6 shows the first-order difference curves of voltage and stress under a low current test. In general, the differential curve of voltage changes greatly in the low and high SOCs, while the differential curve of stress reveals significant fluctuations in moderate SOCs. The changes in stress differential curves are still more obvious than voltage differential curves during battery aging. In a word, the mechanical response together with the electrochemical response can enrich battery aging information.

2.2. Correlation Analysis

Correlation analysis helps in selecting features that have the most significant impact on the target variable since the maximum available capacity directly reflects the health status of the battery. The correlation between each health feature factor and the maximum available capacity was further discussed. The

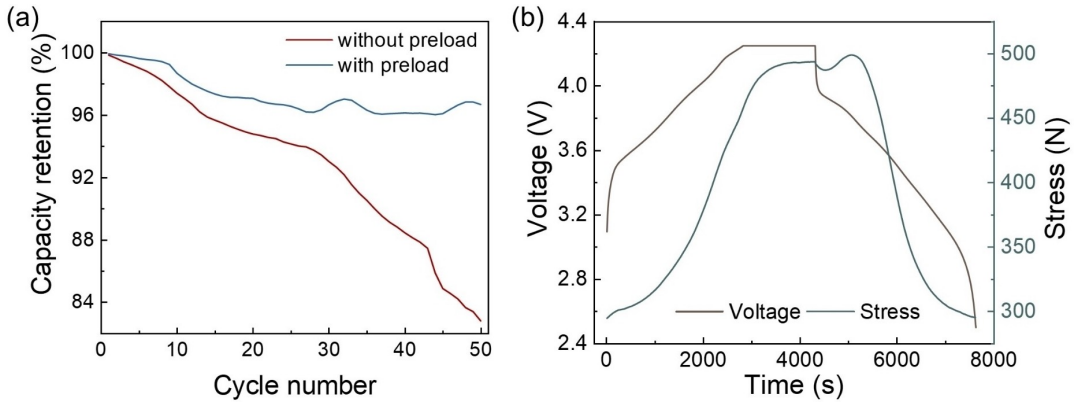

Figure 4. (a) Evolution of capacity with and without preload. (b) Voltage and stress curves in a charging-discharging cycle

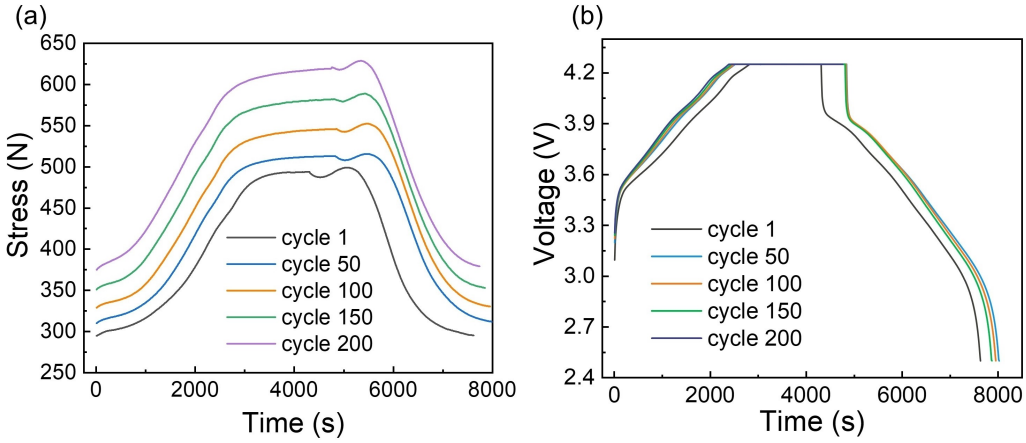

Figure 5. Voltage and stress curves with battery aging process. (a) Stress; (b) Voltage.

Research Article
doi.org/10.1002/batt.202400201
Chemistry Europe
European Chemical Societies Publishing

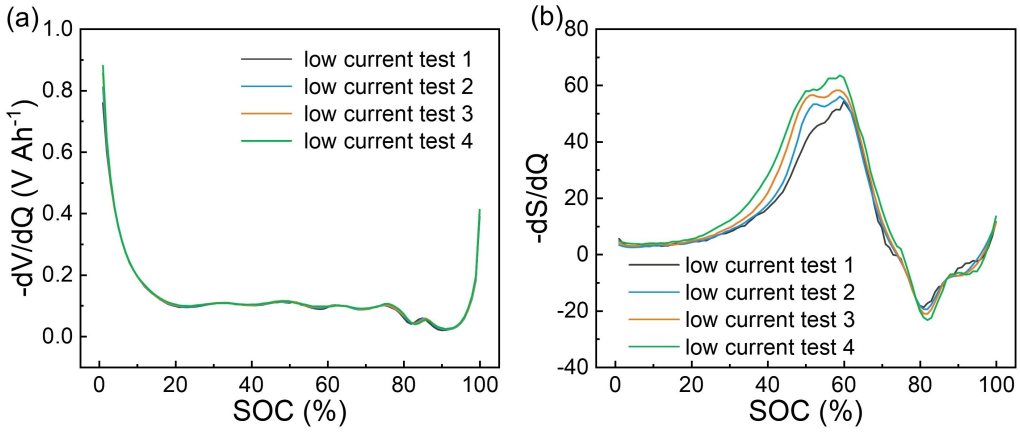

Figure 6. Voltage and stress differential curves with battery aging process: (a) Stress; (b) Voltage.

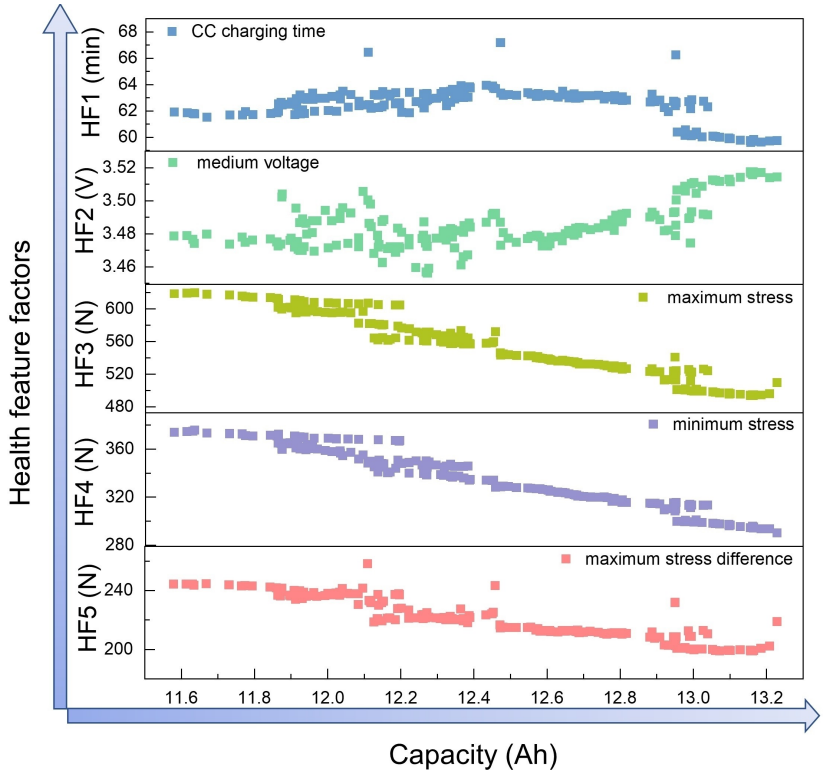

Figure 7. Relation between health feature factors and available capacity.

relationship between capacity and health features is shown in Figure 7. It can be observed that there is a certain relationship between all the extracted health feature factors and the capacity, where the relationship between the mechanical characteristics and the capacity is more obvious than that of the electrochemical characteristics.

The calculation results are shown in Table 3. Although the absolute value of Pearson coefficient of HF1 is the lowest, it was still retained as a health feature factor as the constant-current constant-voltage ratio is an important indicator of the response to the battery state in the CCCV charging strategy.

Table 3. The Pearson correlation coefficient outcomes.

Health feature factors	Pearson correlation coefficient
HF1	−0.318
HF2	0.5953
HF3	−0.9729
HF4	−0.9767
HF5	−0.9255

2.3. Validation of the SOH Estimation Results

The nonlinear relationship between health feature factors and SOH was established by LSTM, where the health feature factors (HF1, HF2, HF3, HF4, HF5) were defined as input and the estimated SOH was defined as output. The LSTM model is trained to minimize the error between the estimated values and the observed SOH values. The estimation results and errors under different cases are illustrated in Figure 8, where the horizontal axis label indicates the cycle number of the battery in the test set.

From the degree of consistency of the results, the LSTM-based estimation method can achieve satisfactory accuracy. The SOH estimation errors of all cases can be restricted within 1.5%, which proves the effectiveness and robustness of the proposed method for batteries with varying aging trajectories. The calculation results of evaluation metrics including *MAE*, *MAPE*, *RMSE*, and R^2 are reported in Table 4. In case 1, the value of R^2 is the highest, indicating that the overall fit of the curve is the best. Other estimation errors of case 3 are the smallest, for which the minimum *MAE*, *MAPE*, and *RMSE* are 0.15, 0.19%, and 0.91 respectively. Overall, the results reveal that when combined with mechanical response, the estimation model has a broader application for calculating the SOH.

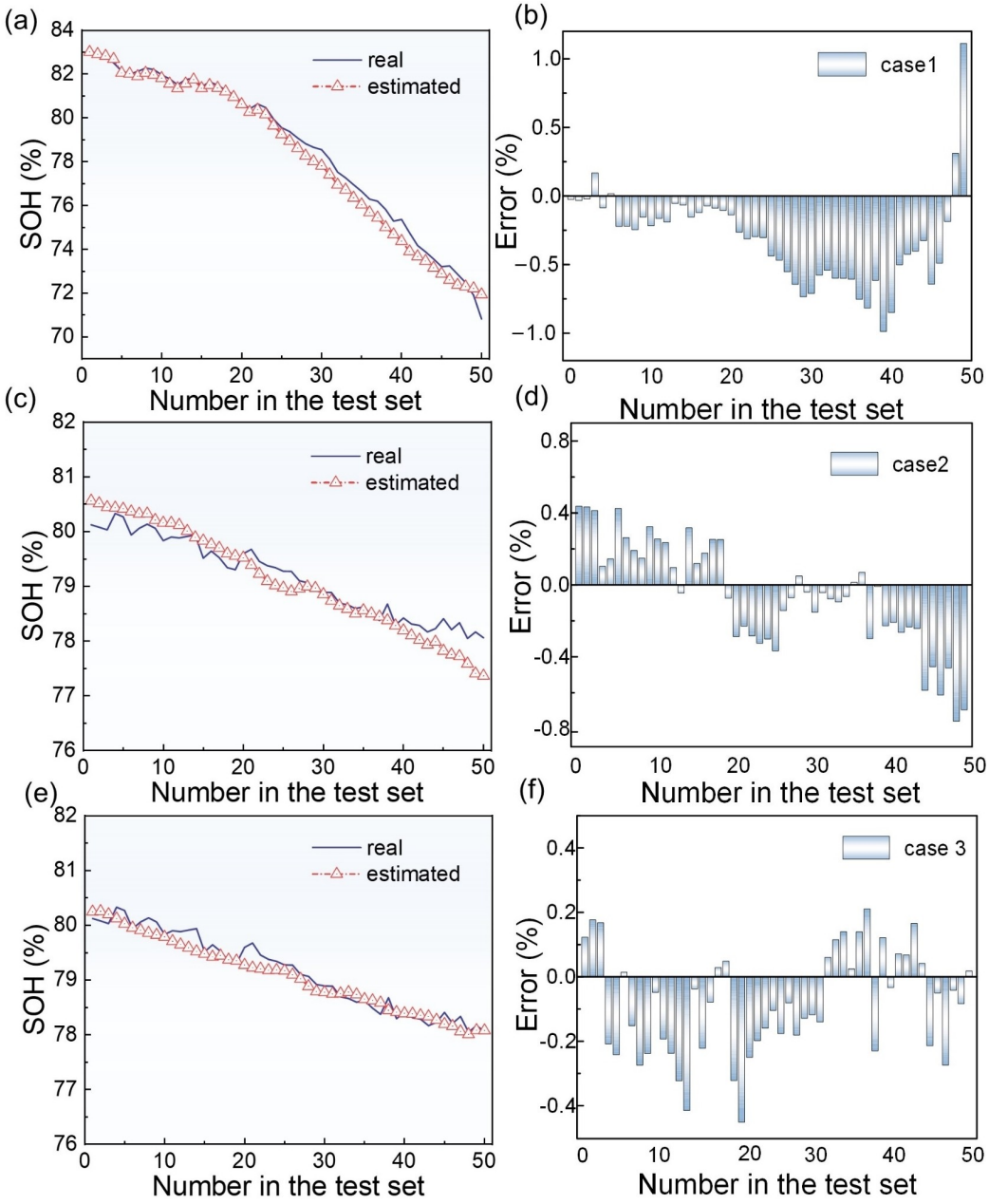

Figure 8. SOH estimation results and errors under different cases. (a)–(b) case 1; (c)–(d) case 2; (e)–(f) case 3.

Table 4. Error analysis of SOH estimation under different cases.

Error	*MAE*	*MAPE* (%)	*RMSE*	R^2
case 1	0.3728	0.486	2.3118	0.9824
case 2	0.2477	0.3133	1.5166	0.8157
case 3	0.1529	0.1927	0.9142	0.933

3. Conclusions

This work has presented an advanced SOH estimation method integrating mechanical and electrical characteristics of battery degradation. To begin, the datasets including voltage and stress signals are constructed based on aging tests in different scenarios. Then five key parameters extracted from the stress and voltage profiles are selected as health feature factors, which indirectly reflect the degree of battery aging. Subsequently, the battery SOH estimation is performed using LSTM network under different cases. Results show that the mechanical-electrical feature-based SOH estimation method can well track the true value in all cases. On the laboratory test data of pouch-type lithium-ion batteries, the SOH minimum estimation errors of *MAE*, *MAPE*, *RMSE*, and R^2 are 0.15, 0.19%, 0.91. and 0.93, respectively. This result demonstrates that the proposed method has achieved satisfactory performance. The attempts made in this paper by using mechanical-electrical rather than an electrical signal to estimate SOH have broadened the diversity of SOH estimation methods for pouch lithium-ion batteries.

Acknowledgements

We thank the funding support from National Key R&D Program of China (2023YFB2408100), Anhui Provincial Natural Science Foundation of China (BJ2090130065), and the Fundamental Research Funds for the Central Universities (WK2090000055).

Conflict of Interests

One Chinese patent (No. 202211410285.7) related to this work has been filed.

Data Availability Statement

The data that support the findings of this study are available from the corresponding author upon reasonable request.

Keywords: State of health estimation · Stress measurement · Pouch-type lithium-ion battery · Health feature extraction · Machine learning

[1] International Energy Agengy, *Global EV Outlook 2023*, OECD, **2023**.
[2] M. S. Hossain Lipu, M. A. Hannan, T. F. Karim, A. Hussain, M. H. M. Saad, A. Ayob, M. S. Miah, T. M. Indra Mahlia, *J. Cleaner Prod.* **2021**, *292*, 126044.
[3] G. Vennam, A. Sahoo, S. Ahmed, *J. Energy Storage* **2022**, *52*, 104720.
[4] M. Berecibar, I. Gandiaga, I. Villarreal, N. Omar, J. Van Mierlo, P. Van den Bossche, *Renewable Sustainable Energy Rev.* **2016**, *56*, 572–587.
[5] Z. Li, S. Shen, Z. Zhou, Z. Cai, W. Gu, F. Zhang, *J. Energy Storage* **2023**, *62*, 106927.
[6] M. S. Hossain Lipu, S. Ansari, M. S. Miah, S. T. Meraj, K. Hasan, A. S. M. Shihavuddin, M. A. Hannan, K. M. Muttaqi, A. Hussain, *J. Energy Storage* **2022**, *55*, 105752.
[7] W. Zhenpo, *J. Mech. Eng.* **2023**, *59*, 151.
[8] J. Li, K. Adewuyi, N. Lotfi, R. G. Landers, J. Park, *Appl. Energy.* **2018**, *212*, 1178–1190.
[9] R. Xiong, Y. Zhang, H. He, X. Zhou, M. G. Pecht, *IEEE Trans. Ind. Electron.* **2018**, *65*, 1526–1538.
[10] Y. Li, M. Abdel-Monem, R. Gopalakrishnan, M. Berecibar, E. Nanini-Maury, N. Omar, P. van den Bossche, J. Van Mierlo, *J. Power Sources* **2018**, *373*, 40–53.
[11] X. Li, Z. Wang, J. Yan, *J. Power Sources* **2019**, *421*, 56–67.
[12] G. Liu, X. Zhang, Z. Liu, *Energy* **2022**, *259*, 124851.
[13] H. H. Goh, Z. Lan, D. Zhang, W. Dai, T. A. Kurniawan, K. C. Goh, *J. Energy Storage* **2022**, *50*, 104646.
[14] G. Ma, S. Xu, B. Jiang, C. Cheng, X. Yang, Y. Shen, T. Yang, Y. Huang, H. Ding, Y. Yuan, *Energy Environ. Sci.* **2022**, *15*, 4083–4094.
[15] A. Mukhopadhyay, B. W. Sheldon, *Prog. Mater. Sci.* **2014**, *63*, 58–116.
[16] C. Peabody, C. B. Arnold, *J. Power Sources* **2011**, *196*, 8147–8153.
[17] X. Su, B. Sun, J. Wang, H. Ruan, W. Zhang, Y. Bao, *J. Energy Storage* **2023**, *68*, 107793.
[18] R. Li, W. Li, A. Singh, D. Ren, Z. Hou, M. Ouyang, *Energy Storage Mater.* **2022**, *52*, 395–429.
[19] J. Cannarella, C. B. Arnold, *J. Power Sources* **2014**, *245*, 745–751.
[20] J. Cannarella, C. B. Arnold, *J. Power Sources* **2014**, *269*, 7–14.
[21] S. Mohan, Y. Kim, J. B. Siegel, N. A. Samad, A. G. Stefanopoulou, *J. Electrochem. Soc.* **2014**, *161*, A2222–A2231.
[22] H. Dai, C. Yu, X. Wei, Z. Sun, *Energy* **2017**, *129*, 16–27.
[23] P. Xu, J. Li, Q. Xue, F. Sun, *J. Energy Storage* **2022**, *50*, 104559.
[24] L. Gong, Z. Zhang, Y. Li, X. Li, K. Sun, P. Tan, *J. Energy Storage* **2022**, *55*, 105720.
[25] N. A. Samad, Y. Kim, J. B. Siegel, A. G. Stefanopoulou, *J. Electrochem. Soc.* **2016**, *163*, A1584–A1594.
[26] P. Mohtat, S. Lee, J. B. Siegel, A. G. Stefanopoulou, *J. Power Sources* **2019**, *427*, 101–111.
[27] L. De Sutter, G. Berckmans, M. Marinaro, M. Wohlfahrt-Mehrens, M. Berecibar, J. Van Mierlo, *J. Power Sources* **2020**, *451*, 227774.
[28] P. Mohtat, S. Lee, J. B. Siegel, A. G. Stefanopoulou, *J. Power Sources* **2022**, *518*, 230714.
[29] M. A. Perez Estevez, F. V. Conte, C. Tremonti, M. Renzi, *J. Energy Storage* **2023**, *64*, 107186.
[30] M. Zhang, W. Li, L. Zhang, H. Jin, Y. Mu, L. Wang, *Inf. Sci. (Ny)* **2023**, *639*, 118737.
[31] Z. Xi, R. Wang, Y. Fu, C. Mi, *Appl. Energy* **2022**, *305*, 117962.
[32] M. Lin, J. Wu, J. Meng, W. Wang, J. Wu, *Energy* **2023**, *268*, 126706.

Manuscript received: March 24, 2024
Revised manuscript received: May 6, 2024
Accepted manuscript online: May 6, 2024
Version of record online: June 14, 2024